0090-9556/10/3808-1267–1276$20.00
DRUG METABOLISM AND DISPOSITION
Vol. 38, No. 8
32797/3607238
DMD 38:1267–1276, 2010
Printed in U.S.A.
Copyright © 2010 by The American Society for Pharmacology and Experimental Therapeutics

Formation Pathways of γ-Butyrolactone from the Furan Ring of Tegafur during Its Conversion to 5-Fluorouracil

Ikuo Yamamiya, Kunihiro Yoshisue, Eiji Matsushima, and Sekio Nagayama

Tokushima Research Center, Taiho Pharmaceutical Co., Ltd., Tokushima, Japan

Received February 15, 2010; accepted May 11, 2010

ABSTRACT:

Tegafur (FT) is a 5-fluorouracil (5-FU) prodrug that has been clinically used for various cancer chemotherapies. The following metabolites of FT were identified in patients: 5-FU, fluoro-β-alanine, and γ-butyrolactone (GBL) and its acidic form, γ-hydroxybutyrate (GHB). GBL/GHB, which is probably generated from the furan ring of FT, inhibits tumor cell angiogenesis, contributing to the antitumor effect of FT-based therapies. In the present study, we identified the metabolites formed from the furan ring of FT by CYP2A6 and thymidine phosphorylase (TPase) using 2,4-dinitrophenylhydrazine derivatization procedures and clarified the metabolic pathway of FT to GBL/GHB. Succinaldehyde (SA) and 4-hydroxybutanal (4-OH-BTL) were produced as the metabolites because of the cleavage of the furan ring of FT during its conversion to 5-FU in cDNA-expressed CYP2A6 and purified TPase, respectively; however, GBL/GHB was hardly detected in cDNA-expressed CYP2A6 and purified TPase. GBL/GHB was formed after human hepatic microsomes or cDNA-expressed CYP2A6 mixed with cytosol were incubated with FT. Furthermore, 4-OH-BTL was converted to GBL/GHB in the microsomes and cytosol. These results suggest that GBL/GHB is generated from FT through the formation of SA and 4-OH-BTL but not directly from FT. Furthermore, the amount of 5-FU and GBL/GHB formed in the hepatic S9 was markedly decreased in the presence of a CYP2A6 inhibitor, suggesting that GBL/GHB may be mainly generated through the CYP2A6-mediated formation of SA.

Tegafur [5-fluoro-1-(2-tetrahydrofuryl)-2,4(1*H*,3*H*)-pyrimidinedione] (FT) is a prodrug of 5-fluorouracil (5-FU) and has been used clinically for various cancer chemotherapies. FT is metabolized to its active form 5-FU in the liver. 5-FU inhibits the growth of cancer cells by being incorporated into RNA or by inhibiting thymidylate synthase, which is the only de novo source of thymidylate required for DNA synthesis (Ullman and Kirsch, 1979; Danenberg and Lockshin, 1982). Previous studies have revealed that the conversion of FT to 5-FU is catalyzed by cytochrome P450s and thymidine phosphorylase (TPase) in the microsomes and cytosol, respectively (Kono et al., 1981; El Sayed and Sadée, 1982, 1983; Kawata et al., 1984, 1987; Sugata et al., 1986; Komatsu et al., 2001). Furthermore, it has been reported that CYP2A6 is mainly responsible for the bioactivation of FT to 5-FU in human hepatic microsomes (Ikeda et al., 2000; Komatsu et al., 2000). The following metabolites of FT have been identified in the plasma and urine of patients: 5-FU, fluoro-β-alanine, and γ-butyrolactone (GBL) and its acidic form, γ-hydroxybutyrate (GHB) (Benvenuto et al., 1978; Au and Sadée, 1980; Peters et al., 2003; Emi et al., 2007). The metabolism of 5-FU to fluoro-β-alanine involves multiple steps, including the action of various enzymes such as dihydropyrimidine dehydrogenase (DPD), and, subsequently, it is excreted into urine. GBL/GHB, which is present endogenously (Bessman and Fishbein, 1963; Tabakoff and von Wartburg, 1975), is considered to be generated from the furan ring of FT. In addition, it has been reported that GBL/GHB inhibits vascular endothelial growth factor (VEGF)-mediated angiogenesis in tumor cells and thus contributes to the antitumor effect of FT-based therapies (Yonekura et al., 1999; Basaki et al., 2000; Nagai et al., 2008). During the conversion of FT to 5-FU, the furan ring of FT is thought to undergo hydroxylation at the 2′- or 5′-position, followed by the sequential decomposition to 5-FU because both the hydroxy metabolites of FT are chemically unstable (Lin et al., 1979). During the decomposition of chemically unstable 2′- and 5′-hydroxy metabolites of FT to 5-FU, the furan rings of these metabolites are speculated to be converted to GBL and succinaldehyde (SA), respectively (Lin et al., 1979; El Sayed and Sadée, 1983). Furthermore, 4-hydroxybutanal (4-OH-BTL) is generated by the spontaneous hydrolytic cleavage at the N1–C2′ bond of the furan moiety of FT (Au and Sadée, 1980). Although GBL/GHB was detected in vitro after the incubation of FT with mouse and rabbit hepatic homogenates (Au and Sadée, 1980), the metabolic pathways of the furan ring of FT to form GBL/GHB remain to be clarified.

In this study, we identified the metabolites formed from the furan ring of FT during its conversion to 5-FU mediated by CYP2A6 and TPase and clarified the metabolic pathway of FT leading to the formation of GBL/GHB in humans. We used the

Article, publication date, and citation information can be found at http://dmd.aspetjournals.org.

doi:10.1124/dmd.110.032797.

ABBREVIATIONS: FT, tegafur; 5-FU, 5-fluorouracil; TPase, thymidine phosphorylase; GBL, γ-butyrolactone; GHB, γ-hydroxybutyrate; DPD, dihydropyrimidine dehydrogenase; VEGF, vascular endothelial growth factor; SA, succinaldehyde; 4-OH-BTL, 4-hydroxybutanal; DNPH, 2,4-dinitrophenylhydrazine; CDHP, 5-chloro-2, 4-dihydroxypyridine; TPI, 5-chloro-6-(2-iminopyrrolidin-1-yl) methyl-2,4(1*H*,3*H*)-pyrimidinedione hydrochloride; TCP, tranylcypromine hydrochloride; QqTOF, hybrid quadrupole time of flight; LC, liquid chromatography; MS/MS, tandem mass spectrometry; ESI, electrospray ionization; MRM, multiple reaction monitoring; CE, collision energy; UPLC, ultraperformance liquid chromatography; IS, internal standard; GC, gas chromatography; MS, mass spectrometry; UFT, uracil-tegafur.

Downloaded from dmd.aspetjournals.org at ASPET Journals on April 6, 2015

2,4-dinitrophenylhydrazine (DNPH) derivatization procedure, which is widely used in the analysis of aldehydes and ketones (Zwiener et al., 2002; Andreoli et al., 2003), to detect unstable metabolites formed from the furan ring of FT.

Materials and Methods

Chemicals. FT, 5-chloro-2,4-dihydroxypyridine (CDHP), 5-chloro-6-(2-iminopyrrolidin-1-yl) methyl-2,4(1*H*,3*H*)-pyrimidinedione hydrochloride (TPI), and 4-OH-BTL were synthesized at Taiho Pharmaceutical Co. (Saitama, Japan). Succinaldehyde disodium bisulfite was purchased from Tokyo Chemical Industry Co. (Tokyo, Japan). 5-FU, β-NAD$^+$, glucose 6-phosphate, GBL-d_6, DNPH, tranylcypromine hydrochloride (TCP), phenanthridine, menadione sodium bisulfite, and 4-methylpyrazole were purchased from Sigma-Aldrich (St. Louis, MO). Magnesium chloride hexahydrate, disulfiram, coumarin, thymidine, thymine, acetaldehyde, ethanol, and GBL were purchased from Wako Pure Chemical Industries (Osaka, Japan). β-NADP$^+$ and glucose-6-phosphate dehydrogenase were purchased from Oriental Yeast Co. (Tokyo, Japan). Other chemicals used were of the highest grade commercially available.

Enzymes. Human liver samples were purchased from XenoTech, LLC (Kansas City, KS). Membranes prepared from *Escherichia coli* expressing CYP2A6 (Bactosomes) were obtained from Cypex Ltd (Dundee, UK). Control membranes expressed only the vector. Purified TPase from *E. coli* was purchased from Sigma-Aldrich.

Preparation of Standard of DNPH Derivatives. The standard DNPH derivative of SA was prepared using the following procedures. Succinaldehyde disodium bisulfite was dissolved in an HCl aqueous solution. The reaction was initiated by the addition of a 3.1 mg/ml aliquot of DNPH/HCl solution to the SA/HCl aqueous solution, and the mixture was incubated at 37°C for 15 min. Next, the DNPH derivative was extracted with ethyl acetate. The organic layer was dried, and the resultant residue was purified by silica gel column chromatography (Wakogel-C200; Wako Pure Chemical Industries). The molecular structure of the derivative was confirmed by use of a hybrid quadrupole time-of-flight (QqTOF) mass spectrometer and ^{1}H NMR analysis. The standard DNPH-derivative of 4-OH-BTL was also prepared using the same procedure as that used for the preparation of SA-DNPH. 4-OH-BTL was incubated in DNPH/HCl solution at 37°C. The DNPH derivative was extracted with ethyl acetate, and the collected organic layer was evaporated. The derivative of 4-OH-BTL was characterized using its parent ion, and the subsequent fragmentation pattern was characterized using LC-MS/MS.

Assay to Determine the Formations of 5-FU and GBL/GHB from FT in Human Liver Microsomes, Cytosol, or S9. The decrease in the amount of 5-FU formed from FT may be attributed to extensive metabolism of 5-FU by contaminated DPD. Therefore, a potent DPD inhibitor, CDHP, was added to all incubations to inhibit the degradation of 5-FU. The standard reaction mixture contained FT, 1 mM CDHP, and an NADPH-generating system consisting of 1.3 mM β-NADP$^+$, 3.3 mM glucose 6-phosphate, 3.3 mM magnesium chloride, and 0.4 U/ml glucose-6-phosphate dehydrogenase, in 100 mM phosphate buffer-0.1 mM EDTA (pH 7.4). The reactions were initiated by the addition of human hepatic microsomes, cytosol, or S9, after preincubation for 5 min at 37°C. All incubations were performed for 30 min at 37°C. Reactions were stopped by the addition of 3 volumes of ice-cold acetonitrile to the mixtures. After the centrifugation, the supernatant was collected and stored at −80°C until the determinations of 5-FU and GBL. Both microsomes and cytosol were used at a concentration of 1 mg/ml, and S9 was used at a concentration of 2 mg/ml. The spontaneous degradation of FT was evaluated using inactivated S9, which was prepared by boiling it at 100°C for 5 min.

Assay to Determine the Formations of 5-FU, GBL/GHB, SA, and 4-OH-BTL from FT in cDNA-Expressed CYP2A6 or Purified TPase. The standard reaction mixture contained FT and 1 mM CDHP in 100 mM phosphate buffer-0.1 mM EDTA (pH 7.4). To examine CYP2A6-mediated metabolism of FT, cDNA-expressed CYP2A6 and an NADPH-generating system were added to the reaction mixtures. The spontaneous degradation of FT was evaluated using control membranes. To investigate the effect of human liver cytosol on CYP2A6-mediated formations of 5-FU and GBL/GHB, cytosol was added to bacterial membranes containing expressed CYP2A6 or control membranes, and the final concentration was 1 mg/ml. In the case of TPase-mediated metabolism, we used 10.5 U/ml of purified TPase. To determine the spontaneous degradation of FT, we performed the reaction without TPase. The reactions were initiated by the addition of cDNA-expressed CYP2A6 or purified TPase, after preincubation for 5 min at 37°C. The reactions were performed as described for the assay of FT metabolism in human hepatic microsomes, cytosol, and S9. To examine the formation of metabolites from the furan ring of FT, we added a 3.1 mg/ml aliquot of DNPH/HCl solution to the mixture after the reaction, followed by incubation for 15 min at 37°C. Next, DNPH derivatives were extracted with ethyl acetate, and the organic layer was dried under a nitrogen stream. The resultant residue was dissolved in the mobile phase and injected into the LC-MS/MS system.

Assay to Determine the Formation of GBL/GHB from 4-OH-BTL in Human Liver Microsomes or Cytosol. The standard mixture contained 62.5 μM 4-OH-BTL and 1 mg/ml cytosol in 100 mM phosphate buffer-0.1 mM EDTA (pH 7.4). We used β-NAD$^+$ or an NADPH-generating system as cofactors in these assays. The spontaneous degradation of 4-OH-BTL to GBL/GHB was evaluated using inactivated human liver cytosol, which was prepared by boiling it at 100°C for 5 min. After preincubation for 5 min at 37°C, reactions were initiated by the addition of human liver cytosol, followed by incubation for 3 min. Reactions were stopped by mixing the samples with 3 volumes of ice-cold acetonitrile. After the centrifugation, the supernatant was collected and stored at −80°C until the determination of GBL.

Inhibition Study. We determined the effects of inhibitors of CYP2A6 and TPase on the formations of the FT metabolites, including 5-FU, GBL/GHB, SA, and 4-OH-BTL. TCP and TPI were used as inhibitors of CYP2A6 and TPase, respectively (Fukushima et al., 2000; Zhang et al., 2001). Each inhibitor was added to the reaction mixture at a concentration of 10 μM.

We determined the effects of different oxidase inhibitors, disulfiram (an aldehyde dehydrogenase inhibitor), 4-methylpyrazole (an alcohol dehydrogenase inhibitor), and menadione (an aldehyde oxidase inhibitor), on the formation of GBL/GHB from 4-OH-BTL in human hepatic cytosol at a concentration of 100 μM (Pietruszko, 1975; Lam et al., 1997; Lake et al., 2002; Obach et al., 2004). The reactions were performed as described above.

Assay to Determine the Enzyme Activities of Biological Samples (Positive Control). CYP2A6 and TPase activities of biological samples were evaluated by measuring coumarin 7-hydroxylase activity and the formation rate of thymine (from thymidine), respectively. Coumarin 7-hydroxylase activity was determined by a fluorometric assay (Bogaards et al., 2000). The thymine formed from thymidine was measured with high-performance liquid chromatography. The high-performance liquid chromatography analysis was performed with a Prominence LC-20 system (Shimadzu, Kyoto, Japan) equipped with a TSKgel ODS-100V column (4.6 mm i.d. × 150 mm, 3 μm; Tosoh, Tokyo, Japan). The flow rate was 1.0 ml/min, and the column temperature was 25°C. The mobile phases were A (4.5% acetonitrile) and B (acetonitrile). Typical conditions for the elution were as follows: 100% A (0–8 min), 20% A (8.5 min), 20% A (10.5 min), and 100% A (11–25 min). The eluent was monitored at 256 nm to determine thymine and thymidine. The activities of aldehyde dehydrogenase and alcohol dehydrogenase were assayed by monitoring the formation of β-NADH from β-NAD$^+$ at a wavelength of 340 nm during the metabolism of acetaldehyde and ethanol, respectively. The aldehyde oxidase activity was measured using phenanthridine as the substrate, according to the published method (Lake et al., 2002).

Measurement of DNPH Derivatives. The LC-MS/MS system consisted of an HP1100 series liquid chromatograph (Agilent Technologies, Santa Clara, CA) coupled with an API4000 triple-quadrupole mass spectrometer (Applied Biosystems, Foster City, CA) equipped with a Turbo V source and ESI interface. Chromatographic separation of DNPH derivatives was performed on a XBridge C-18 column (4.6 mm i.d. × 150 mm, 5 μm; Waters, Milford, MA) using 10 mM ammonium acetate and acetonitrile under gradient elution conditions at a flow rate of 0.2 ml/min. We used the following gradient programs: 10 mM ammonium acetate-acetonitrile from 70:30 (v/v) to 10:90 (v/v) in 7 min, immediately back to 70:30 (v/v), and then held for 8 min. Oven temperature was maintained at 40°C. TurboIonSpray was used for ionization with negative ion detection for the measurements of DNPH derivatives. The source temperature was set at 600°C, ionization voltage at −4 kV, and orifice potential at −60 V. Multiple reaction monitoring (MRM) was performed in the negative ionization mode, after the reactions, *m/z* 247 to *m/z* 181 (CE 30 eV)

Downloaded from dmd.aspetjournals.org at ASPET Journals on April 6, 2015

for SA-DNPH and *m/z* 267 to *m/z* 152 (CE 30 eV) for 4-OH-BTL-DNPH. Data acquisition was performed using Analyst 1.4.1 software (Applied Biosystems).

QqTOF MS/MS and ^{1}H NMR Analysis. The high mass resolution experiments were performed on a QSTAR Elite hybrid QqTOF mass spectrometer equipped with a TurboIonSpray source (Applied Biosystems). The LC-MS/MS parameters were set as described above. NMR spectra of the synthetic product were obtained on a JM-EX 270 spectrometer (JEOL Ltd., Tokyo, Japan) operating at 270.05 MHz, and chemical shifts were expressed relative to tetramethylsilane.

Measurement of 5-FU and GBL. The concentration of 5-FU was determined using an UPLC-MS/MS system. The UPLC-MS/MS system consisted of a Waters AQUITY ultra-performance liquid chromatograph coupled with a Quattro Premier XE triple-quadrupole mass spectrometer (both from Waters) equipped with a Z-Spray ion source and an ESI interface. Sample separation was performed using a Unison UK-Amino column (2.0 mm i.d. × 100 mm, 3 μm; Imtakt, Kyoto, Japan) at a flow rate of 0.2 ml/min at 40°C. The mobile phase consisted of 10 mM ammonium acetate-acetonitrile (10:90, v/v). MS/MS analysis was performed in negative ionization mode under MRM, using mass transitions, *m/z* 128.6 to *m/z* 41.8 (CE 14 eV) for 5-FU and *m/z* 130.6 to *m/z* 42.8 (CE 14 eV) for internal standard (IS) ($^{15}N_2$-5-FU). MassLynx was used for instrument control and data acquisition. To measure the amount of 5-FU in the biological sample, we mixed 100 μl of the supernatant obtained in the metabolic assays with 50 μl of 500 ng/ml IS-75% acetonitrile solution in an injection vial and then injected 5 μl of the aliquot into the UPLC-MS/MS system. The concentration of GBL was determined using a GC/MS system. GC/MS was performed using a Trace-GC gas chromatograph and AS2000 automatic sampler with a Trace-MS quadrupole mass spectrometer (all equipment from Thermo Fisher Scientific, Waltham, MA). Negative ion chemical ionization was performed using isobutane as the reagent gas. Ionization was initiated at 70 eV with an emission current of 150 mA. The source temperature was 210°C, and the GC interface temperature was 250°C. The GC column was interfaced directly to the ion source. Gas chromatographic separation was performed on a DB-WAX capillary column (30 m × 0.32 mm i.d., film thickness 0.25 mm; J and W Scientific, Folsom, CA). The column temperature was programmed by using the following two-ramp temperature program: the oven was heated at 50°C/min to 280°C and maintained at this temperature until analysis, the oven temperature was then increased at the rate of 20°C/min to 190°C for the first ramp and at the rate of 40°C/min to 250°C for the second ramp, and finally the oven temperature was maintained for 2 min. Xcalibur (version 1.2) was used for instrument control and data acquisition. GBL was partially converted to its acid form, GHB, in chemical equilibrium. Therefore, GBL was measured after the lactonization of GHB under acidic conditions. We used the following procedure for sample preparation for the measurement of GBL/GHB. For in vitro assay, we added a 0.5-ml aliquot of 6 M HCl and 50 μl of IS-methanol solution (2 μg/ml GBL-d_6) to 0.2 ml of the supernatant. After 2 ml of CH_2Cl_2 was added to the above mixture, the mixture was shaken for 10 min and centrifuged at 5°C. The organic layer was pipetted out and transferred to another test tube. CH_2Cl_2 extraction was repeated. The combined organic layer was evaporated under a gentle stream of nitrogen. The concentrated organic layer was transferred to an injection vial, and then 1 μl of aliquot was injected into the GC/MS system. GBL and IS were detected by a selected ion monitoring procedure at *m/z* 85 and *m/z* 90, respectively.

Statistical Analysis. All of the results are presented as the mean ± S.D. Statistical significance was analyzed by Student's *t* test, Dunnet's test, or Tukey's test. SAS (version 6.12 software; SAS Institute, Inc., Cary, NC) was used for all of the statistical analyses.

Results

Enzyme Activities of Biological Samples (Positive Control). The results of the determinations of the enzyme activities of the biological samples and effects of enzyme inhibitors are presented in Table 1. These results served as a positive control in the present investigations and demonstrated that cDNA-expressed CYP2A6, purified TPase, and human liver samples were active. Each typical inhibitor showed more than 80% inhibition against the marker enzyme activity.

Formations of 5-FU and GBL/GHB from FT in cDNA-Expressed CYP2A6 and Purified TPase. Initial studies were performed to investigate the formations of 5-FU and GBL/GHB from FT catalyzed by CYP2A6 or TPase. The formation of 5-FU was observed after the incubation of FT (1 mM) with cDNA-expressed CYP2A6 in the presence of an NADPH-generating system. Moreover, 5-FU was generated from FT (0.25 mM) in purified TPase. We observed a linear and time-dependent increase in the amount of 5-FU formed in both cDNA-expressed CYP2A6 and purified TPase. However, the formation of GBL/GHB was hardly observed in both enzymes.

The effects of CYP2A6 and TPase inhibitors on the conversion of FT to 5-FU are shown in Fig. 1. The addition of a potent CYP2A6 inhibitor, TCP (10 μM), decreased the formation of 5-FU from FT to 42% of the control value (without the inhibitor), and the remaining activity was similar to that in the control membranes. Likewise, the addition of a potent TPase inhibitor, TPI (10 μM), completely inhibited the conversion of FT to 5-FU.

Characterization of DNPH Derivatives. We applied the DNPH derivatization approach to detect SA and 4-OH-BTL in the reaction mixtures. We synthesized the derivatized standards of SA and

TABLE 1

Enzyme activities of biological samples and effects of typical inhibitors

Each value represents the mean ± S.D. (n = 3).

Marker Enzyme	Enzyme Source	Probe Substrate	Inhibitor	Enzyme Activity
CYP2A6 (pmol/min/pmol of P450)	cDNA-expressed	Coumarin		7.1 ± 0.1
			+TCP (10 μM)	0.7 ± 0.2
CYP2A6 (pmol/min/mg)	Microsomes	Coumarin		424.0 ± 30.3
			+TCP (10 μM)	12.0 ± 1.6
CYP2A6 (pmol/min/mg)	S9	Coumarin		262.7 ± 9.7
			+TCP (10 μM)	11.4 ± 0.3
TPase (nmol/min)	Purified TPase	Thymidine		6.6 ± 0.3
			+TPI (10 μM)	N.D.
TPase (nmol/min/mg)	Cytosol	Thymidine		9.0 ± 0.3
			+TPI (10 μM)	N.D.
TPase (nmol/min/mg)	S9	Thymidine		5.5 ± 0.7
			+TPI (10 μM)	N.D.
ALDH (nmol/min/mg)	Cytosol	Acetaldehyde		5.8 ± 0.8
			+Disulfiram (100 μM)	0.4 ± 0.4
ALH (nmol/min/mg)	Cytosol	Ethanol		18.0 ± 1.5
			+4-Methylpyrazole (100 μM)	3.1 ± 0.7
ALO (nmol/min/mg)	Cytosol	Phenanthridine		2.8 ± 0.2
			+Menadione (100 μM)	0.2 ± 0.1

ALDH, aldehyde dehydrogenase; ALH, alcohol dehydrogenase; ALO, aldehyde oxidase; cDNA-expressed, cDNA-expressed CYP2A6; microsomes, human liver microsomes; S9, human liver S9; cytosol, human liver cytosol; N.D., not detected.

Downloaded from dmd.aspetjournals.org at ASPET Journals on April 6, 2015

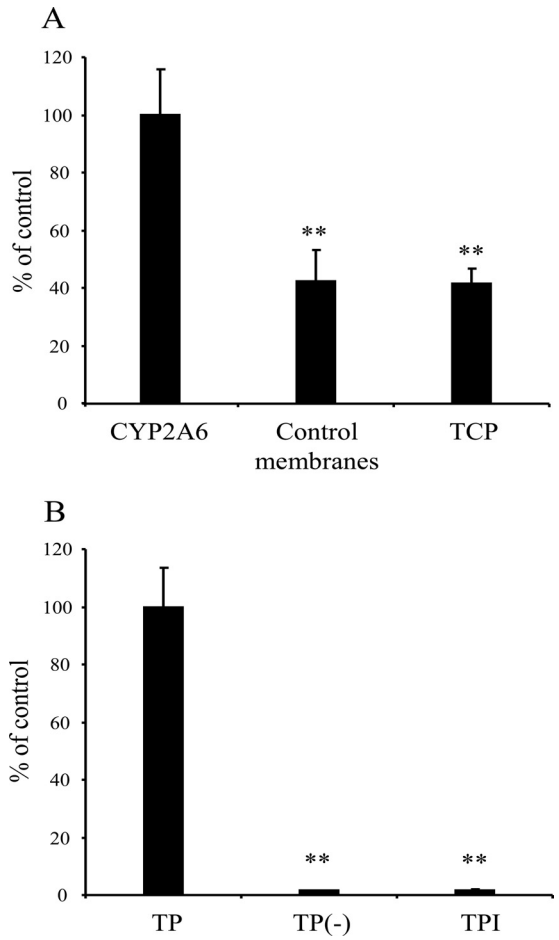

FIG. 1. Effects of inhibitors of CYP2A6 (A) and TPase (B) on the formation of 5-FU in cDNA-expressed CYP2A6 and purified TPase. FT (1 mM for CYP2A6 and 0.25 mM for TPase) was incubated in cDNA-expressed CYP2A6 (25 pmol/ml) or purified TPase (10.5 U/ml) in the absence or presence of inhibitors at 37°C for 30 min. Data are expressed as percentages of the formation of 5-FU in the incubation mixture without inhibitors. Each bar represents the mean ± S.D. ($n = 3$). The formations of 5-FU in cDNA-expressed CYP2A6 and purified TPase were 2.3 ± 0.4 pmol/min/pmol of P450 and 18.9 ± 4.0 pmol/min/U, respectively. **, significantly different ($p < 0.01$) from CYP2A6 or TPase.

4-OH-BTL and characterized their structures. Typical parent and product ion spectra of SA and 4-OH-BTL derivatives were obtained by negative ESI-MS/MS analysis. The ion spectra of 4-OH-BTL-DNPH in the negative ESI ion mode showed a predominant ion $[M - H]^-$ at *m/z* 267, corresponding to the actual molecular weight of the derivative. We observed a predominant ion, $[M - H]^-$ at *m/z* 247 for SA DNPH in the negative ion mode, which was 18 atomic mass units lower than the molecular weight of the expected mono-DNPH attachment derivative at *m/z* 265. The time-of-flight mass analysis revealed that the $[M - H]^-$ ion for SA-DNPH exhibited the molecular composition of $C_{10}H_7N_4O_4$, corresponding to the loss of H_2O molecule from the mono-DNPH attached adduct of $C_{10}H_9N_4O_5$ (Table 2). The formation of SA-DNPH possibly proceeds via the Paal-Knorr pyrrole synthesis reaction (Fig. 2). First, the aldehyde group of SA reacted with DNPH to form the mono-DNPH derivative. Subsequently, a rapid reaction was triggered by a nucleophilic attack on the remaining carbonyl carbon in the amino group of the enamine intermediate, which results in the closed-ring structure, followed by dehydration to form the stable pyrrole compound. The results of QqTOF MS/MS analysis are shown in Table 2; fragmentation of the ion at

TABLE 2

Product ion mass spectra analysis of SA-DNPH using QqTOF MS/MS under the negative ESI condition

An accuracy error threshold of ±5 mDa was set as a limit to the calculation of possible elemental compositions.

	Measured Mass	Calculated Mass	Formula	Electron State
MS^1 $[M - H]^-$	247.0479	247.0472	$C_{10}H_7N_4O_4$	Even
MS^2	229.0372	229.0367	$C_{10}H_5N_4O_3$	Even
MS^2	181.0174	181.0129	$C_6H_3N_3O_4$	Odd
MS^2	164.0142	164.0141	$C_6H_2N_3O_3$	Even
MS^2	151.0180	151.0149	$C_6H_3N_2O_3$	Even
MS^2	135.0232	135.0200	$C_6H_3N_2O_2$	Even
MS^2	120.0116	120.0091	$C_6H_2NO_2$	Even
MS^2	105.0240	105.0220	C_6H_3NO	Odd
MS^2	76.0207	76.0192	C_5H_2N	Even
MS^2	66.0357	66.0349	C_4H_4N	Even

m/z 247 showed typical product ions at *m/z* 181 and *m/z* 66, which were identified as molecules with the molecular formulae, $C_6H_3N_3O_4$ and C_4H_4N, respectively. The radical anion $[M]^-$ at *m/z* 181 was formed by the cleavage of SA-DNPH at the α-amino group of its hydrazine moiety and subjected to further fragmentation. As shown in Table 2, the series of the fragment ions at *m/z* 164, *m/z* 151, *m/z* 135, *m/z* 120, and *m/z* 105 were assigned to $C_6H_2N_3O_3$, $C_6H_3N_2O_3$, $C_6H_2N_2O_2$, $C_6H_2NO_2$, and C_6H_3NO, respectively, by QqTOF MS/MS analysis. These ions were probably formed through subsequent concomitant losses of NO, NO_2, or OH from the product ion at *m/z* 181 by direct bond cleavage and the loss of HNO and others. The other molecular anion $[M]^-$ at *m/z* 66 with the molecular formula, C_4H_4N, was attributed to the pyrrole ring of SA-DNPH. Furthermore, in its ^1H NMR spectrum (270.05 MHz, $CDCl_3$), the characteristic signals at 6.34 (2H, t, $J = 2.5$ Hz) and 6.76 (2H, t, $J = 2.5$ Hz) ppm suggested a symmetric heterocyclic structure of the pyrrole ring, along with the proton signals at 6.34 (1H, d, $J = 9.5$ Hz), 8.25 (1H, dd, $J = 2.5$ and 9.5 Hz), 9.16 (1H, d, $J = 2.5$ Hz), and 10.27 (1H, s) ppm; those were assigned to DNPH moiety. The subsequent detection of DNPH derivatives in biological samples was obtained in MRM, after the reactions *m/z* 247 to *m/z* 181 (CE 30 eV) for SA-DNPH and *m/z* 267 to *m/z* 152 (CE: 30 eV) for 4-OH-BTL-DNPH.

Formations of SA and 4-OH-BTL from FT in cDNA-Expressed CYP2A6 and Purified TPase. To investigate the formations of SA and 4-OH-BTL from FT catalyzed by CYP2A6 or TPase, metabolic studies were conducted using the DNPH derivatization. The formation of DNPH derivatives in the reaction mixtures was confirmed by comparing the retention times of SA-DNPH (8.1 min) and 4-OH-BTL-DNPH (6.8 min) with those of their corresponding standards. We compared the peak area of each DNPH derivative obtained from the MRM analysis under the different conditions. TCP and TPI exerted inhibitory effects on the formations of SA-DNPH and 4-OH-BTL-DNPH in cDNA-expressed CYP2A6 or purified TPase as shown in Fig. 3. After FT (5 mM) was incubated in cDNA-expressed CYP2A6, SA-DNPH was observed as a much larger peak than that observed in other assays, and the formation of 4-OH-BTL-DNPH in cDNA-expressed CYP2A6 was similar to that in control membranes. As shown in Fig. 3, a small amount of SA-DNPH observed in the absence of FT was derived from DNPH. The addition of TCP (10 μM) completely decreased the formation of SA-DNPH in cDNA-expressed CYP2A6, whereas the formation of 4-OH-BTL-DNPH was unaffected (Fig. 3A). Furthermore, the formation of 4-OH-BTL in control membranes was similar to that in cDNA-expressed CYP2A6, which suggests that 4-OH-BTL was generated by the spontaneous degradation of FT.

Downloaded from dmd.aspetjournals.org at ASPET Journals on April 6, 2015

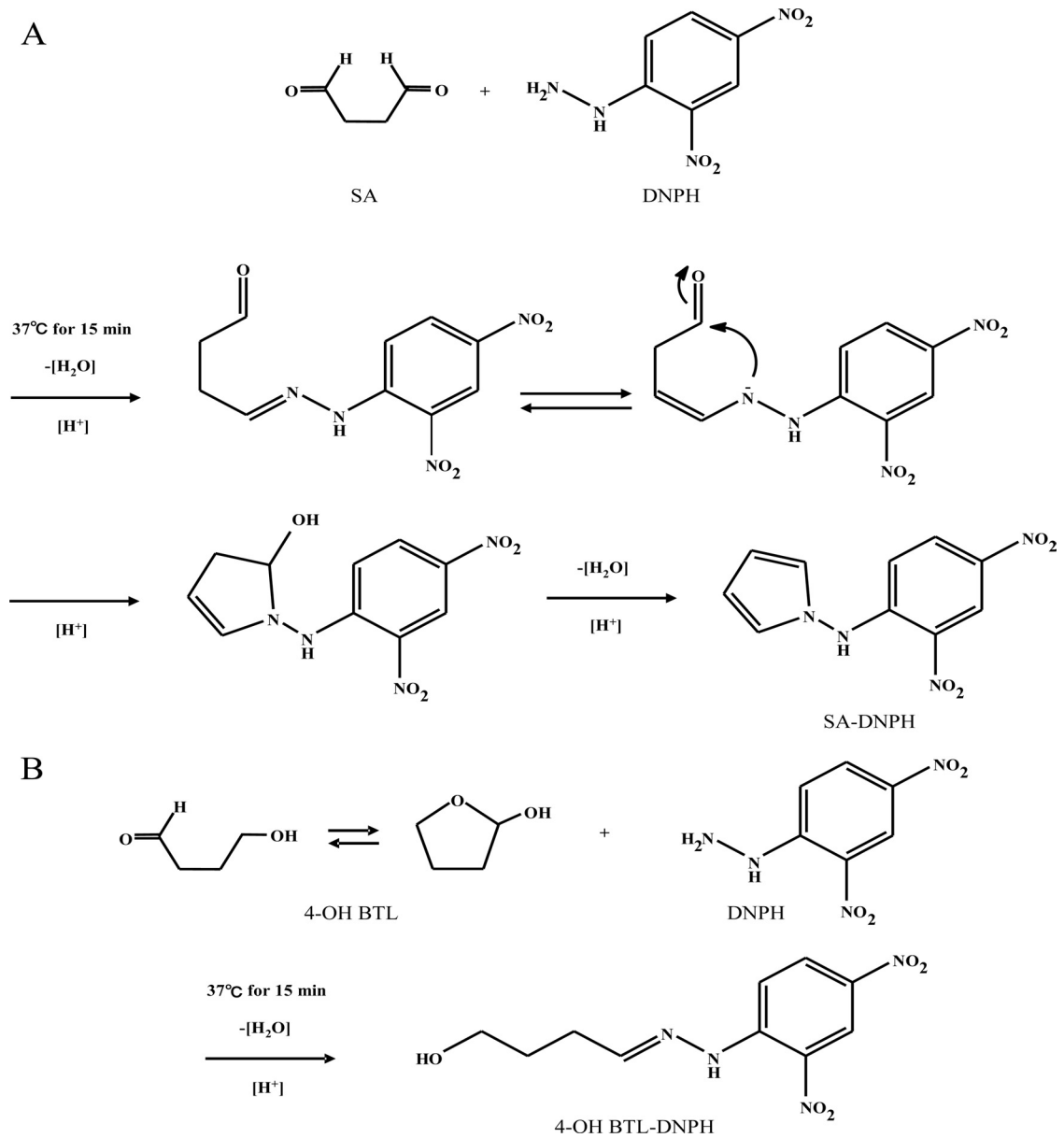

FIG. 2. Proposed derivatization pathways for SA (A) and 4-OH-BTL (B) with DNPH.

After FT was incubated in purified TPase, the peak of 4-OH-BTL was much higher than that observed in other reaction mixtures. Furthermore, the amount of SA-DNPH formed was similar to that formed in the mixture incubated without purified TPase or FT. The addition of TPI (10 μM) resulted in complete inhibition of the formation of 4-OH-BTL from FT in TPase (Fig. 3B).

Formations of 5-FU and GBL/GHB in cDNA-Expressed CYP2A6 or Human Liver Cytosol. The effect of addition of human liver cytosol on the formation of GBL/GHB was assessed to investigate the conversion of SA and 4-OH-BTL to GBL/GHB during the metabolism of FT to 5-FU. The formations of 5-FU and GBL/GHB from FT (1 mM) in cDNA-expressed CYP2A6 or human liver cytosol are shown in Fig. 4. The formation of 5-FU was observed in all reaction mixtures, whereas GBL/GHB was not generated in the absence of human liver cytosol. The addition of cytosol increased the amount of 5-FU formed in cDNA-expressed CYP2A6 (from 9.9 $\pm$ 0.8 to 13.2 $\pm$ 0.7 pmol/min) and control membranes (from 2.6 $\pm$ 0.1 to 4.8 $\pm$ 0.2 pmol/min). The amount of 5-FU generated from FT in human liver cytosol was 4.6 $\pm$ 0.1 pmol/min. After FT was incubated in cDNA-expressed CYP2A6 with human liver cytosol, the amount of GBL/GHB generated was higher (4.1 $\pm$ 0.2 pmol/min) than that in control membranes with human liver cytosol (2.4 $\pm$ 0.2 pmol/min), which indicates that metabolites such as SA and 4-OH-BTL that are generated from the furan ring of FT in cDNA-expressed CYP2A6 are converted to GBL/GHB by cytosolic enzymes.

Formation of GBL/GHB from 4-OH-BTL in Human Liver Cytosol and Microsomes. We investigated the involvement of human liver microsomes and cytosol in the conversion of 4-OH-BTL to GBL/GHB. Formation of GBL/GHB from 4-OH-BTL (67 μM) in human liver cytosol and microsomes is shown in Fig. 5. In human liver cytosol, 4-OH-BTL was converted to GBL/GHB, and the additions of β-NAD^+ and NADPH enhanced the formation of GBL/GHB. We used the inhibitors at much higher concentrations than those of their K_i and IC_{50} values reported (Pietruszko, 1975; Lam et al., 1997; Obach et al., 2004). The typical inhibitors, disulfiram, 4-methylpyrazole, and menadione showed more than an 80% inhibitory effect on

Downloaded from dmd.aspetjournals.org at ASPET Journals on April 6, 2015

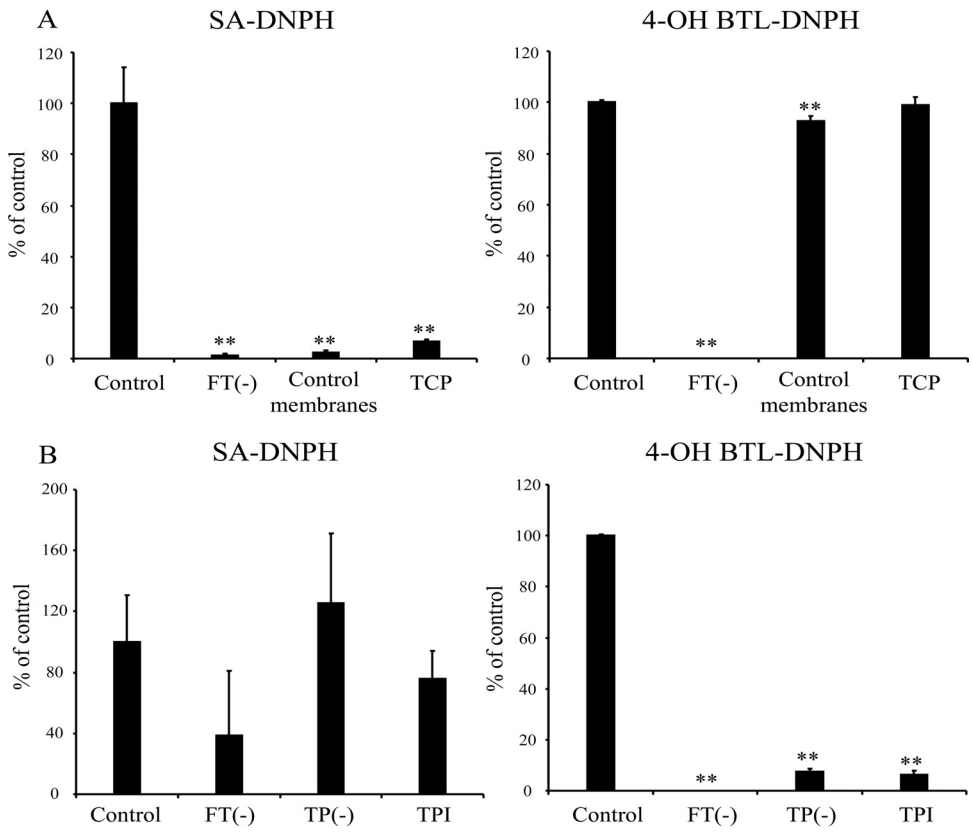

FIG. 3. Formations of SA and 4-OH-BTL from FT in cDNA-expressed CYP2A6 (A) or purified TPase (B). FT was incubated in cDNA-expressed CYP2A6 (25 pmol/ml) or purified TPase (10.5 U/ml) in the absence or presence of the inhibitor at 37°C. After the reaction, the derivatives of metabolites were prepared using DNPH. Data are expressed as percentages of the formations of SA-DNPH and 4-OH-BTL-DNPH in the incubation mixture of FT without inhibitors (control). Each bar represents the mean ± S.D. ($n = 3$). **, significantly different ($p < 0.01$) from control in each reaction. The retention times of peaks of DNPH derivatives in incubations were preliminary, determined by coelution of biological samples with the derivatized standards.

marker metabolic enzymes in cytosol at the concentration of 100 μM (Table 1).

The formation of GBL/GHB was inhibited by the addition of disulfiram (100 μM) and menadione (100 μM), approximately by 72 and 45%, respectively, whereas the addition of 4-methylpyrazole (100 μM) had little effect on the formation of GBL/GHB (Fig. 5A). The formation of GBL/GHB from 4-OH-BTL in hepatic microsomes was similar to its spontaneous formation in the inactivated cytosol. The addition of β-NAD^+ resulted in an increase in the formation of GBL/GHB in human liver microsomes; the amount of GBL/GHB formed was similar to that in hepatic cytosol.

Formations of 5-FU and GBL/GHB from FT in Human Liver Microsomes, Cytosol, or S9. To clarify the metabolism of FT in human liver, the formations of 5-FU and GBL/GHB from FT were investigated in human liver microsomes, cytosol, and S9. The formations of 5-FU and GBL/GHB from FT (1 mM) in hepatic microsomes, cytosol, or S9 after incubation with CYP2A6 and TPase inhibitors are shown in Fig. 6, A and B. In human liver microsomes, the amounts of 5-FU and GBL/GHB generated from FT were 38.1 ± 3.2 and 5.3 ± 0.7 pmol/min, respectively; furthermore, TCP (10 μM) showed 74 and 87% inhibition against the formation of 5-FU and GBL/GHB in hepatic microsomes, respectively. The amounts of 5-FU and GBL/GHB generated from FT in hepatic cytosol were 6.0 ± 0.1 and 2.7 ± 0.3 pmol/min, respectively. TPI (10 μM) slightly decreased the formation of 5-FU in hepatic cytosol to a level similar to that for the inactivated S9. In hepatic S9, the amounts of 5-FU and GBL/GHB generated from FT were 46.0 ± 3.0 and 7.4 ± 0.9 pmol/min, respectively. TCP showed approximately 70% inhibition of the formations of 5-FU and GBL/GHB, whereas TPI had little effect. In inactivated S9, we did not observe the formation of GBL/GHB. Figure 6, C and D, shows the effects of various oxidase inhibitors on the formations of 5-FU and GBL/GHB in human liver microsomes, cytosol, and S9. Disulfiram and menadione inhibited the formation of 5-FU in microsomes by 68 and 87%, respectively. The amount of 5-FU formed in S9 was also significantly decreased to 44 and 14% of the control values by the additions of disulfiram and menadione, respectively. Furthermore, we observed similar results on the formation of GBL/GHB in microsomes and S9. On the other hand, disulfiram showed complete inhibition against the formation of GBL/GHB in the cytosol without affecting the amount of 5-FU formed.

Discussion

GBL/GHB, the metabolite possibly formed from the furan ring of FT, suppresses the VEGF-induced chemotactic migration and tube formation in human umbilical vein endothelial cells stimulated at the IC_{50} of 0.31 μM (26.7 ng/ml) (Basaki et al., 2001). It has been reported that uracil-tegafur (UFT), which is an oral fluoropyrimidine formed by the combination of uracil and FT at a molar ratio of 4:1, has an antiangiogenic effect. Emi et al. (2007) measured the plasma concentration of GBL/GHB in gastric cancer patients, before and after the administration of UFT. The endogenous plasma concentration of GBL/GHB in patients was 16.8 ± 4.0 ng/ml. The mean maximum plasma concentration of GBL/GHB after the administration of UFT was 147.5 ng/ml, which was 5 times higher than its IC_{50} described above. Furthermore, at 4 h after the administration of UFT, the plasma concentration of GBL/GHB (78.0 ng/ml) was three times higher than its IC_{50} of 26.7 ng/ml. Other reports reveal that there is an inverse correlation between the serum levels of GBL/GHB and VEGFs before and after UFT therapy (Nagai et al., 2008). Thus, the antiangiogenesis effects of UFT may be attributed to the action of GBL/GHB, which specifically acts against VEGF-induced angiogenesis. Therefore, GBL/GHB was expected to play an important role in FT-based chemotherapies; however, the mechanism of metabolic cleavage of the furan ring of FT to form GBL/GHB remains to be clarified.

Downloaded from dmd.aspetjournals.org at ASPET Journals on April 6, 2015

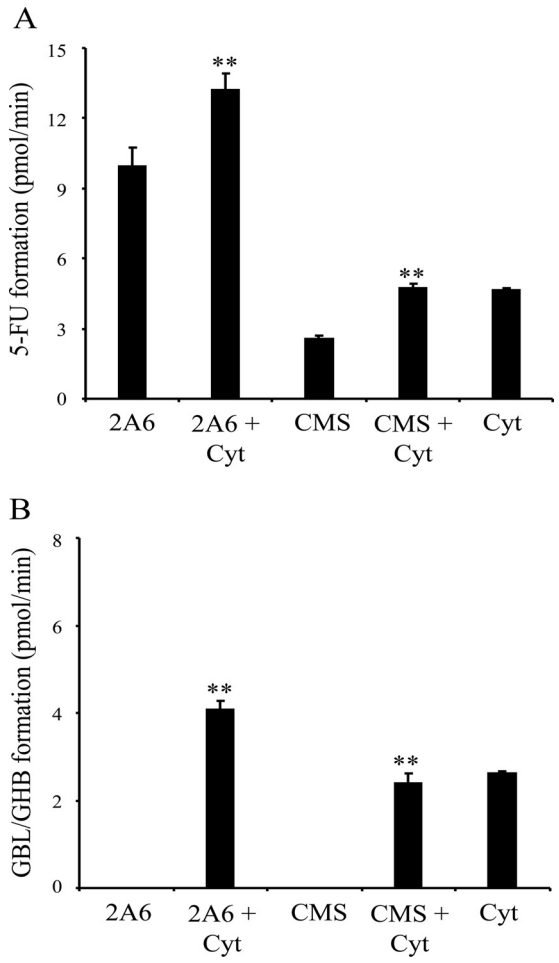

FIG. 4. The formations of 5-FU (A) and GBL/GHB (B) from FT in cDNA-expressed CYP2A6 or human liver cytosol. FT (1 mM) was incubated in cDNA-expressed CYP2A6 (2A6), CYP2A6 with human liver cytosol (2A6 + Cyt), control membranes (CMS), control membranes with cytosol (CMS + Cyt), or cytosol (Cyt) at 37°C for 30 min. Each bar represents the mean ± S.D. ($n = 3$). **, significantly different ($p < 0.01$) from the incubation without cytosol in each reaction.

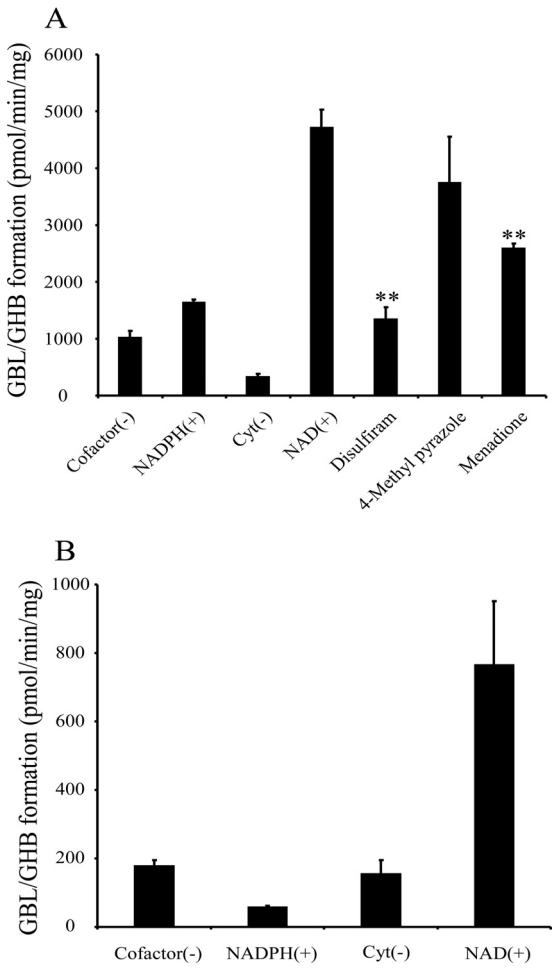

FIG. 5. Formation of GBL/GHB from 4-OH-BTL in cytosol (A) or microsomes (B). 4-OH-BTL (67 μM) was incubated in the cytosol (0.3 mg/ml) or microsomes (0.5 mg/ml) in the absence or presence of cofactors at 37°C for 3 min. Each inhibitor was added to the incubation mixture at a final concentration of 100 μM. Data are expressed as percentages of the formation of 5-FU in the incubation mixture without inhibitors. Each bar represents the mean ± S.D. ($n = 3$). **, significantly different ($p < 0.01$) from the incubation with β-NAD$^+$ in cytosol.

Results from previous studies indicate that 2′- and 5′-hydroxy metabolites of FT are immediately decomposed to 5-FU, because of their chemical instability and that their furan rings would concomitantly be converted to GBL or SA (Lin et al., 1979; El Sayed and Sadée, 1983). However, the metabolic pathways of the furan ring of FT have remained unclear under physiological conditions.

In the present study, we identified the metabolites from the furan ring of FT during its CYP2A6 or TPase-mediated conversion to 5-FU. 5-FU was generated from FT, whereas the formation of GBL/GHB was not observed after the incubation of FT with both cDNA-expressed CYP2A6 and purified TPase. This result indicates that the hydroxylation of FT at the 2′-position does not occur, which results in the formation of GBL/GHB in both enzymes, because the 2′-hydroxy metabolite of FT can be directly converted to GBL/GHB. The chemical derivatization using hydrazine reagents has been reported to improve the sensitivity of detection of poorly ionic carbonyl compounds with MS and overcome the reactive and volatile nature of aliphatic chain aldehydes and ketones (Vogel et al., 2000). To identify the metabolites from the furan ring of FT, such as SA and 4-OH-BTL, which are short-chain dialdehyde and semialdehyde compounds, we used the DNPH derivatization method. The structure of the DNPH derivative of SA was identified as an anilino pyrrole structure by QqTOF MS/MS and ^{1}H NMR analysis. This finding is in agreement with the previous report, which shows that 1,4-diketones reacted with DNPH to form (*N*-2,4-dinitroanilino) pyrroles under the acidic condition (Binns and Brettle, 1966). The 4-OH-BTL-DNPH yielded the parent ion with the expected molecular weight of the mono-DNPH-attached derivative previously reported (Chen et al., 1978). In cDNA-expressed CYP2A6, SA and 4-OH-BTL were generated from FT during its conversion to 5-FU. TCP, a potent CYP2A6 inhibitor, completely inhibited the formation of SA, but it had no effect on the formation of 4-OH-BTL. Furthermore, the formation of 4-OH-BTL in control membranes was similar to that in cDNA-expressed CYP2A6, which indicates that 4-OH-BTL was generated by the spontaneous degradation of FT. These results suggest that FT is hydroxylated at the 5′-position by CYP2A6, resulting in the formation of 5-FU. On the other hand, the furan ring of FT was converted to 4-OH-BTL but not SA by TPase. Thus, the hydrolytic cleavage of the furan ring of FT at the N1–C2′ bond may be catalyzed by TPase, which results in the formation of 4-OH-BTL.

In this study, we showed that GBL/GHB is not directly generated from FT by CYP2A6 and TPase. However, the formation of GBL/GHB has been reported after the incubation of FT with animal hepatic homogenate. In addition, previous studies revealed that GBL/GHB was detected in the plasma of patients in the form

Downloaded from dmd.aspetjournals.org at ASPET Journals on April 6, 2015

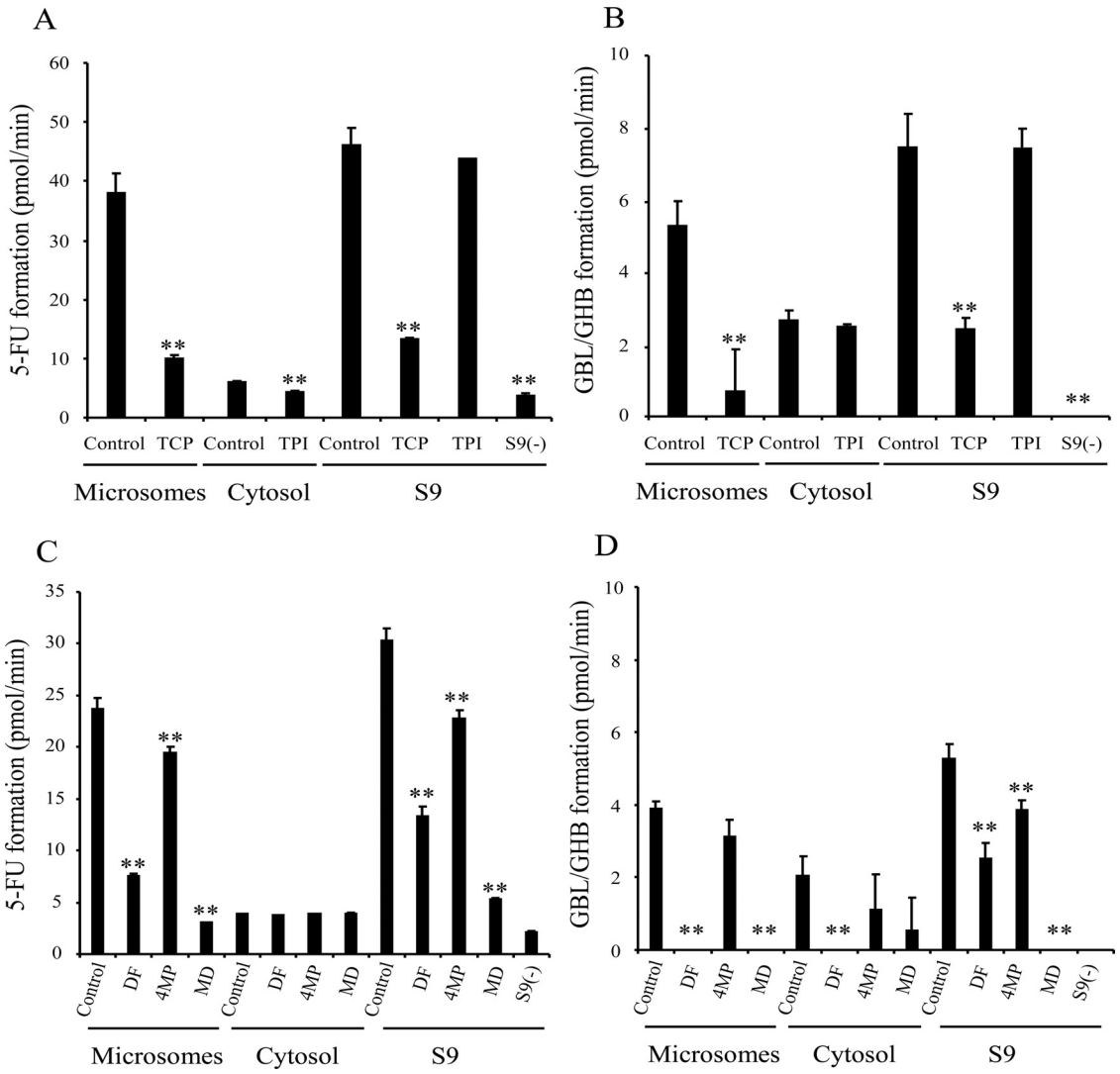

FIG. 6. Formations of 5-FU and GBL/GHB from FT in human hepatic microsomes, cytosol, or S9. Effects of TCP and TPI on the formations of 5-FU (A) and GBL/GHB (B), and disulfiram (DF), 4-methylpyrazole (4MP), and menadione (MD) on the formations of 5-FU (C) and GBL/GHB (D). FT (1 mM) was incubated in microsomes, cytosol, or S9 with an NADPH-generating system and CDHP (1 mM) at 37°C for 30 min in the absence or presence of inhibitors. Each point represents the mean ± S.D. ($n = 3$). **, significantly different ($p < 0.01$) from control in each material.

of a metabolite from the furan ring of FT. Consequently, we investigated the metabolic pathways of SA and 4-OH-BTL in human hepatic samples. 4-OH-BTL occurs as an intermediate during the conversion of 1,4-butanediol to GBL/GHB (Roth and Giarman, 1969). SA is an oxidized form of succinic semialdehyde, which is an endogenous compound and can be reduced to GBL/GHB by GHB synthase (Lyon et al., 2007). Therefore, SA and 4-OH-BTL generated from the furan ring of FT are thought to be converted to GBL/GHB under physiological conditions. In the present study, the addition of cytosol increased the amounts of 5-FU and GBL/GHB formed in cDNA-expressed CYP2A6. The increase in the formation of 5-FU may be attributed to TPase in the cytosol, considering that TPI decreased the formation of 5-FU in the cytosol to a level similar to that of its spontaneous formation in the inactivated S9, which suggests that TPase is responsible for the metabolism of FT in the cytosol. After the addition of cytosol, the amount of GBL/GHB formed in cDNA-expressed CYP2A6 was much greater than that in control membranes with cytosol. Furthermore, the formation of GBL/GHB in human hepatic microsomes was inhibited by TCP. These findings suggest that SA from the furan ring of FT is converted to GBL/GHB in the cytosol and microsomes. Likewise, 4-OH-BTL was converted to GBL/GHB in the cytosol and microsomes. Our study with different inhibitors revealed that aldehyde dehydrogenase and aldehyde oxidase were mainly involved in the conversion of 4-OH-BTL to GBL/GHB in the cytosol. In addition, the amount of GBL/GHB formed from 4-OH-BTL in the cytosol with β-NAD^+, which is a cofactor necessary for aldehyde dehydrogenase in catalyzing the oxidation of aldehydes, was considerably higher than that in microsomes, which suggests that cytosolic dehydrogenases would mainly contribute to the oxidation of 4-OH-BTL to GBL/GHB. These inhibitors strongly inhibited the formation of 5-FU in microsomes and S9, whereas its formation in the cytosol was not affected. The metabolite of disulfiram, diethyldithiocarbamate, and menadione efficiently inhibit CYP2A6 and NADPH-dependent cytochrome P450 reductase, respectively, in microsomes (Sadowski et al., 1986; Ono et al., 1996), which would result in the decrease of the formation of 5-FU in the present study. The amount of GBL/GHB formed in the cytosol was decreased by addition of disulfiram without inhibiting the formation of 5-FU, which indicates that

Downloaded from dmd.aspetjournals.org at ASPET Journals on April 6, 2015

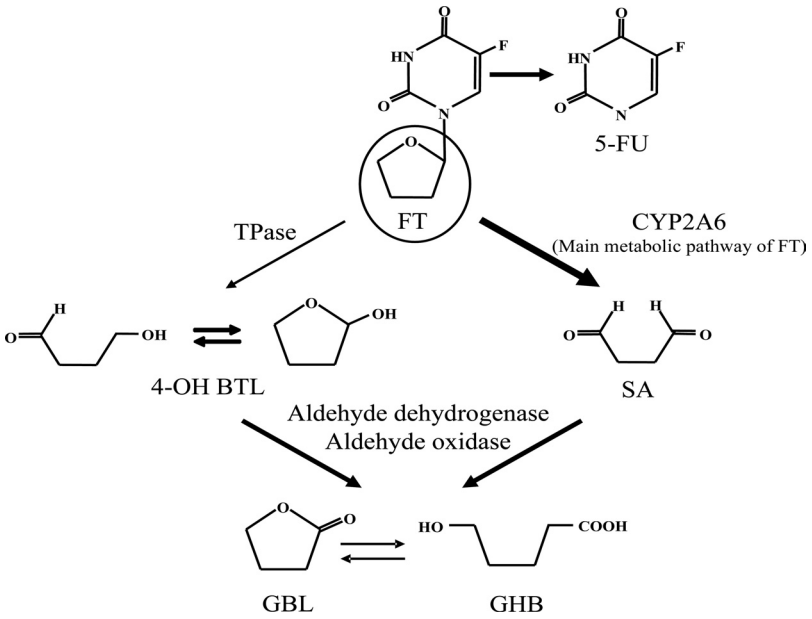

FIG. 7. Proposed metabolic pathway of FT.

4-OH-BTL formed during the conversion of FT to 5-FU can be converted to GBL/GHB by aldehyde dehydrogenase. In human hepatic S9, the addition of TCP exerted a strong inhibitory effect on the formation of 5-FU, whereas TPI had little effect, which suggests that in the human liver, CYP2A6, but not TPase, is mainly responsible for the conversion of FT to 5-FU. We observed similar results during the formation of GBL/GHB in the hepatic S9, which indicates that the CYP2A6-mediated metabolic pathway of the furan ring of FT, followed by the sequential conversion of SA to GBL/GHB may contribute mainly to the formation of GBL/GHB under physiological conditions. The studies on endogenous GBL/GHB catabolism have shown the oxidation of GBL/GHB to succinic semialdehyde by GHB dehydrogenase, followed by its oxidation to succinate by succinic semialdehyde dehydrogenase in mitochondria (Kaufman et al., 1979). Therefore, GBL/GHB generated after the administration of FT may be finally metabolized to succinate in mitochondria in vivo.

The proposed metabolic pathway of the furan ring of FT is shown in Fig. 7. In this study, we clarified that SA and 4-OH-BTL were generated from the furan ring of FT by CYP2A6 and TPase, respectively, during its conversion to 5-FU. Furthermore, we showed that these metabolites were converted to GBL/GHB in human hepatic samples. In human liver, the CYP2A6-mediated conversion of the furan ring of FT to SA, followed by the oxidation to GBL/GHB, may be the main pathway responsible for the formation of GBL/GHB.

References

Andreoli R, Manini P, Corradi M, Mutti A, and Niessen WM (2003) Determination of patterns of biologically relevant aldehydes in exhaled breath condensate of healthy subjects by liquid chromatography/atmospheric chemical ionization tandem mass spectrometry. *Rapid Commun Mass Spectrom* **17:**637–645.

Au JL and Sadée W (1980) Activation of Ftorafue [*R,S*-1-(tetrahydro-2-furanyl)-5-fluorouracil] to 5-fluorouracil and γ-butyrolactone. *Cancer Res* **40:**2814–2819.

Basaki Y, Aoyagi K, Chikahisa L, Miyadera K, Hashimoto A, Yonekura K, Okabe S, Shibata J, Wierzba K, and Yamada Y (2000) UFT and its metabolites inhibit cancer-induced angiogenesis. Via a VEGF-related pathway. *Oncology (Williston Park)* **14:**68–71.

Basaki Y, Chikahisa L, Aoyagi K, Miyadera K, Yonekura K, Hashimoto A, Okabe S, Wierzba K, and Yamada Y (2001) γ-Hydroxybutyric acid and 5-fluorouracil, metabolites of UFT, inhibit the angiogenesis induced by vascular endothelial growth factor. *Angiogenesis* **4:**163–173.

Benvenuto JA, Lu K, Hall SW, Benjamin RS, and Loo TL (1978) Disposition and metabolism of 1-(tetrahydro-2-furanyl)-5-fluorouracil (ftorafur) in humans. *Cancer Res* **38:**3867–3870.

Bessman SP and Fishbein WN (1963) γ-Hydroxybutyrate, a normal brain metabolite. *Nature* **200:**1207–1208.

Binns TD and Brettle R (1966) The reactions of some 1,4-diketones with 2,4-dinitrophenylhydrazine. *J Chem Soc C* 341–343.

Bogaards JJ, Bertrand M, Jackson P, Oudshoorn MJ, Weaver RJ, van Bladeren PJ, and Walther B (2000) Determining the best animal model for human cytochrome P450 activities: a comparison of mouse, rat, rabbit, dog, micropig, monkey and man. *Xenobiotica* **30:**1131–1152.

Chen CB, McCoy GD, Hecht SS, Hoffmann D, and Wynder EL (1978) High pressure liquid chromatographic assay for α-hydroxylation of N-nitrosopyrrolidine by isolated rat liver microsomes. *Cancer Res* **38:**3812–3816.

Danenberg PV and Lockshin A (1982) Thymidylate synthetase-substrate complex formation. *Mol Cell Biochem* **43:**49–57.

El Sayed YM and Sadée W (1982) Metabolic activation of ftorafur [*R,S*-1-(tetrahydro-2-furanyl)-5-fluorouracil]: the microsomal oxidative pathway. *Biochem Pharmacol* **31:**3006–3008.

El Sayed YM and Sadée W (1983) Metabolic activation of *R,S*-1-(tetrahydro-2-furanyl)-5-fluorouracil (ftorafur) to 5-fluorouracil by soluble enzymes. *Cancer Res* **43:**4039–4044.

Emi Y, Sumiyoshi Y, Oki E, Kakeji Y, Fukui Y, and Maehara Y (2007) Pharmacokinetics of γ-hydroxybutyric acid (GHB) and γ-butyrolactone (GBL), the anti-angiogenic metabolites of oral fluoropyrimidine UFT, in patients with gastric cancer. *Fukuoka Igaku Zasshi* **98:**418–424.

Fukushima M, Suzuki N, Emura T, Yano S, Kazuno H, Tada Y, Yamada Y, and Asao T (2000) Structure and activity of specific inhibitors of thymidine phosphorylase to potentiate the function of antitumor 2′-deoxyribonucleosides. *Biochem Pharmacol* **59:**1227–1236.

Ikeda K, Yoshisue K, Matsushima E, Nagayama S, Kobayashi K, Tyson CA, Chiba K, and Kawaguchi Y (2000) Bioactivation of tegafur to 5-fluorouracil is catalyzed by cytochrome P-450 2A6 in human liver microsomes in vitro. *Clin Cancer Res* **6:**4409–4415.

Kaufman EE, Nelson T, Goochee C, and Sokoloff L (1979) Purification and characterization of an $NADP^+$-linked alcohol oxido-reductase which catalyzes the interconversion of γ-hydroxybutyrate and succinic semialdehyde. *J Neurochem* **32:**699–712.

Kawata S, Minami Y, Tarui S, Marunaka T, Okamoto M, and Yamano T (1984) Cytochrome P-450-dependent oxidative cleavage of 1-(tetrahydro-2-furanyl)-5-fluorouracil to 5-fluorouracil. *Jpn J Pharmacol* **36:**43–49.

Kawata S, Noda S, Imai Y, Tamura S, Saitoh R, Miyoshi S, Minami Y, and Tarui S (1987) Hepatic conversion of 1-(tetrahydro-2-furanyl)-5-fluorouracil into 5-fluorouracil in patients with hepatocellular carcinoma. *Gastroenterol J* **22:**55–62.

Komatsu T, Yamazaki H, Shimada N, Nagayama S, Kawaguchi Y, Nakajima M, and Yokoi T (2001) Involvement of microsomal cytochrome P450 and cytosolic thymidine phosphorylase in 5-fluorouracil formation from tegafur in human liver. *Clin Cancer Res* **7:**675–681.

Komatsu T, Yamazaki H, Shimada N, Nakajima M, and Yokoi T (2000) Roles of cytochromes P450 1A2, 2A6, and 2C8 in 5-fluorouracil formation from tegafur, an anticancer prodrug, in human liver microsomes. *Drug Metab Dispos* **28:**1457–1463.

Kono A, Hara Y, and Matsushima Y (1981) Enzymatic formation of 5-fluorouracil from 1-(tetrahydro-2-furanyl)-5-fluorouracil (tegafur) in human tumor tissues. *Chem Pharm Bull (Tokyo)* **29:**1486–1488.

Lake BG, Ball SE, Kao J, Renwick AB, Price RJ, and Scatina JA (2002) Metabolism of zaleplon by human liver: evidence for involvement of aldehyde oxidase. *Xenobiotica* **32:**835–847.

Lam JP, Mays DC, and Lipsky JJ (1997) Inhibition of recombinant human mitochondrial and cytosolic aldehyde dehydrogenases by two candidates for the active metabolites of disulfiram. *Biochemistry* **36:**13748–13754.

Lin AJ, Benjamin RS, Rao PN, and Loo TL (1979) Synthesis and biological activities of ftorafur metabolites. 3′- and 4′-hydroxyftorafur. *J Med Chem* **22:**1096–1100.

Lyon RC, Johnston SM, Watson DG, McGarvie G, and Ellis EM (2007) Synthesis and catabolism of γ-hydroxybutyrate in SH-SY5Y human neuroblastoma cells: role of the aldo-keto reductase AKR7A2. *J Biol Chem* **282:**25986–25992.

Nagai N, Mukai K, Hirata E, Jin HH, Komatsu M, and Yunokawa M (2008) UFT and its metabolite γ-butyrolactone (GBL) inhibit angiogenesis induced by vascular endothelial growth factor in advanced cervical carcinoma. *Med Oncol* **25:**214–221.

Obach RS, Huynh P, Allen MC, and Beedham C (2004) Human liver aldehyde oxidase: inhibition by 239 drugs. *J Clin Pharmacol* **44:**7–19.

Ono S, Hatanaka T, Hotta H, Satoh T, Gonzalez FJ, and Tsutsui M (1996) Specificity of substrate

Downloaded from dmd.aspetjournals.org at ASPET Journals on April 6, 2015

and inhibitor probes for cytochrome P450s: evaluation of in vitro metabolism using cDNA-expressed human P450s and human liver microsomes. *Xenobiotica* **26:**681–693.

Peters GJ, Noordhuis P, Van Kuilenburg AB, Schornagel JH, Gall H, Turner SL, Swart MS, Voorn D, Van Gennip AH, Wanders J, et al. (2003) Pharmacokinetics of S-1, an oral formulation of ftorafur, oxonic acid and 5-chloro-2,4-dihydroxypyridine (molar ratio 1:0.4:1) in patients with solid tumors. *Cancer Chemother Pharmacol* **52:**1–12.

Pietruszko R (1975) Human liver alcohol dehydrogenase-inhibition of methanol activity by pyrazole, 4-methylpyrazole, 4-hydroxymethylpyrazole and 4-carboxypyrazole. *Biochem Pharmacol* **24:**1603–1607.

Roth RH and Giarman NJ (1969) Conversion in vivo of γ-aminobutyric to γ-hydroxybutyric acid in the rat. *Biochem Pharmacol* **18:**247–250.

Sadowski IJ, Wright JA, Ollmann D, and Israels LG (1986) Menadione inhibition of benzo-(*a*)pyrene metabolism in whole cells, microsomes and reconstituted systems. *Int J Biochem* **18:**565–568.

Sugata S, Kono A, Hara Y, Karube Y, and Matsushima Y (1986) Partial purification of a thymidine phosphorylase from human gastric cancer. *Chem Pharm Bull (Tokyo)* **34:**1219–1222.

Tabakoff B and von Wartburg JP (1975) Separation of aldehyde reductases and alcohol dehydrogenase from brain by affinity chromatography: metabolism of succinic semialdehyde and ethanol. *Biochem Biophys Res Commun* **63:**957–966.

Ullman B and Kirsch J (1979) Metabolism of 5-fluorouracil in cultured cells. Protection from 5-fluorouracil cytotoxicity by purines. *Mol Pharmacol* **15:**357–366.

Vogel M, Büldt A, and Karst U (2000) Hydrazine reagents as derivatizing agents in environmental analysis—a critical review. *Fresenius J Anal Chem* **366:**781–791.

Yonekura K, Basaki Y, Chikahisa L, Okabe S, Hashimoto A, Miyadera K, Wierzba K, and Yamada Y (1999) UFT and its metabolites inhibit the angiogenesis induced by murine renal cell carcinoma, as determined by a dorsal air sac assay in mice. *Clin Cancer Res* **5:**2185–2191.

Zhang W, Kilicarslan T, Tyndale RF, and Sellers EM (2001) Evaluation of methoxsalen, tranylcypromine, and tryptamine as specific and selective CYP2A6 inhibitors in vitro. *Drug Metab Dispos* **29:**897–902.

Zwiener C, Glauner T, and Frimmel FH (2002) Method optimization for the determination of carbonyl compounds in disinfected water by DNPH derivatization and LC-ESI-MS-MS. *Anal Bioanal Chem* **372:**615–621.

Address correspondence to: Ikuo Yamamiya, Tokushima Research Center, Taiho Pharmaceutical Co., Ltd., 224-2, Ebisuno, Hiraishi, Kawauchi-cho, Tokushima 771-0194, Japan. E-mail: i-yamamiya@taiho.co.jp

Downloaded from dmd.aspetjournals.org at ASPET Journals on April 6, 2015